



# Technical feasibility of semiautomatic three-dimensional threshold-based cardiac computed tomography quantification of left ventricular mass

Hyun Woo Goo<sup>1</sup>

Received: 1 July 2018 / Revised: 17 September 2018 / Accepted: 31 October 2018 / Published online: 23 November 2018  
© Springer-Verlag GmbH Germany, part of Springer Nature 2018

## Abstract

**Background** Semiautomatic three-dimensional (3-D) threshold-based cardiac computed tomography (CT) quantification has not been attempted for left ventricular mass.

**Objective** To evaluate the technical feasibility of semiautomatic 3-D threshold-based cardiac CT quantification of left ventricular mass in patients with various degrees of left ventricular hypertrophy.

**Materials and methods** In 99 patients, cardiac CT was utilized to quantify ventricular volume and mass by using a semiautomatic 3-D threshold-based method. Left ventricular mass values were compared between the end-systole and the end-diastole. Volumetric parameters were compared among three left ventricular hypertrophy groups (definite, borderline, none). The reproducibility was assessed. The *t*-test, one-way analysis of variance and Pearson correlation were used.

**Results** There were no technical failures. The left ventricular mass between the two sessions exhibited a small mean difference of  $2.3 \pm 1.1\%$  (mean  $\pm$  standard deviation). The indexed mass values were significantly higher at the end-systole than at the end-diastole ( $71.4 \pm 42.9$  g/m<sup>2</sup> vs.  $65.9 \pm 43.3$  g/m<sup>2</sup>,  $P < 0.001$ ), with significant correlation ( $R = 0.99$ ,  $P < 0.001$ ). The definite group ( $83.5 \pm 41.3$  g/m<sup>2</sup>) showed statistically significantly higher indexed mass values than the borderline and none groups ( $64.7 \pm 26.9$  and  $55.6 \pm 23.9$  g/m<sup>2</sup>, respectively;  $P < 0.03$ ), while demonstrating no statistically significant difference between the latter two groups ( $P > 0.05$ ). Left ventricular volume-mass and mass-volume ratios could be calculated in all three groups.

**Conclusion** CT quantification of left ventricular mass using semiautomatic 3-D threshold-based segmentation is feasible with high reproducibility and the mass values and its ratios with ventricular volumes may be used in patients with various degrees of left ventricular hypertrophy.

**Keywords** Children · Computed tomography · Heart · Image post processing · Left ventricular hypertrophy · Left ventricular mass · Repeatability · Threshold-based segmentation · Young adults

## Introduction

Left ventricular hypertrophy is an independent predictor of adverse cardiovascular events [1]. Therefore, it is of critical importance to measure left ventricular mass accurately not only for initial risk stratification, but also for post-treatment evaluation. For the measurement, M-mode or two-dimensional (2-D) echocardiography has been utilized, but the accuracy is

inherently limited by geometrical assumption [2]. To overcome the limitation, three-dimensional (3-D) echocardiography has been advocated with a comparable accuracy to cardiac magnetic resonance imaging (MRI); however, the accurate left ventricular mass cannot be calculated due to insufficient image quality in up to one-third of cases [3]. In left ventricular mass quantification using cardiac MRI, there has been a debate on including the papillary muscles and trabeculations [4, 5]. It is noteworthy that 2-D simplified contouring excluding the papillary muscles and trabeculations from the left ventricular myocardium substantially underestimates left ventricular mass. A threshold-based segmentation method therefore may provide more accurate left ventricular mass.

A 3-D threshold-based segmentation method is desirable to reduce the errors associated with a 2-D method [6] and cardiac

✉ Hyun Woo Goo  
ghw68@hanmail.net

<sup>1</sup> Department of Radiology and Research Institute of Radiology, Asan Medical Center, University of Ulsan College of Medicine, 88, Olympic-ro 43-gil, Songpa-gu, Seoul 05505, South Korea

computed tomography (CT) can provide an excellent 3-D data set for this volumetric analysis. Recently, a semiautomatic 3-D threshold-based segmentation method could be successfully applied to a 3-D cardiac CT data set for ventricular volume measurements [7–9]. However, its technical feasibility in left ventricular mass quantification remains to be determined. Therefore, this study aimed to evaluate the technical feasibility of a semiautomatic 3-D threshold-based cardiac CT segmentation method for left ventricular mass quantification in patients with various degrees of left ventricular hypertrophy.

## Materials and methods

This retrospective study was approved by the local institutional review board and the requirement for informed consent was waived.

### Study population

Between January 2013 and April 2016, 99 consecutive patients (median age: 27.0 months, range: 2 days–28 years; M:F=63:36) who underwent cardiac CT examinations using a second-generation dual-source scanner (SOMATOM Definition Flash; Siemens Healthineers, Forchheim, Germany) were included in this study. CT volumetry was performed to quantify ventricular volume and mass. The study population had various cardiac diseases, including coarctation of the aorta ( $n=13$ ), Williams syndrome ( $n=11$ ), tetralogy of Fallot ( $n=9$ ), interrupted aortic arch ( $n=8$ ), complete transposition of the great arteries ( $n=8$ ), double outlet right ventricle ( $n=5$ ), atrial septal defect ( $n=5$ ), congenitally corrected transposition of the great arteries ( $n=5$ ), critical aortic stenosis ( $n=4$ ), bicuspid aortic valve ( $n=4$ ), ventricular septal defect ( $n=4$ ), status post heart transplantation ( $n=3$ ), hypoplastic left heart syndrome variant ( $n=3$ ), pulmonary atresia ( $n=3$ ), Kawasaki disease ( $n=2$ ), hypertrophic cardiomyopathy ( $n=2$ ), Takayasu arteritis ( $n=1$ ), right cervical aortic arch ( $n=1$ ), congenital subaortic stenosis ( $n=1$ ), atrioventricular septal defect ( $n=1$ ), Loeys-Dietz syndrome ( $n=1$ ), idiopathic mid aortic syndrome ( $n=1$ ), suspected coronary artery anomaly ( $n=1$ ), left ventricular apical hypoplasia ( $n=1$ ), suspected pulmonary arteriovenous fistula ( $n=1$ ) and idiopathic left ventricular dilation ( $n=1$ ). The body surface area ( $m^2$ ) at the cardiac CT was recorded from electronic medical records to calculate indexed parameters.

### Cardiac CT

Fundamental scan parameters of cardiac CT were as follows:  $2 \times 64 \times 0.6$ -mm slices with the z-flying focal spot technique, a 0.28-s gantry rotation time, a 75-ms temporal resolution, a 0.75-mm slice width and a 0.4-mm reconstruction interval.

A combined tube current modulation (CARE Dose 4D; Siemens Healthineers, Forchheim, Germany) was used in all CT scans. Electrocardiography (ECG) electrodes were placed outside the thoracic region as much as possible to reduce metal artifacts and potential adverse effects on tube current modulation. Because isocentering of a patient in a CT gantry is crucial to optimally use tube current modulation, a radiology technologist adjusted each patient position at the isocenter and an additional radiolucent pad was placed upon the CT table for a small child to compensate for low vertical positions even at the maximum CT table height [10].

For ECG-synchronized data acquisition, breath-hold retrospectively ECG-gated spiral scan in 39 patients, free-breathing combined prospectively ECG- and respiratory-triggered sequential scan in 37 patients and free-breathing prospectively ECG-triggered sequential scan was used in 23 patients. End-systolic phase was obtained in 95 patients, end-diastolic phase in 25 patients and mid-diastolic phase in 3 patients. Paired end-systolic and end-diastolic phases were available in 24 patients. To reduce radiation dose, a biphasic chest pain protocol, in which 50% lower tube current was used outside the heart, was utilized for retrospectively ECG-gated spiral scan, as previously described [11]. Of free-breathing children, respiratory triggering was added to ECG-triggered sequential scanning in patients  $>5$  kg in body weight in whom respiratory motion was large enough to degrade image quality of cardiac CT. Additional respiratory triggering was obtained with a pressure-sensing belt of a respiratory gating system (AZ-733 V; Anzai Medical Co., Tokyo, Japan) as previously described [12, 13]. As a result, the patients scanned with combined triggering tended to be older than those scanned with prospective ECG-triggering (Table 1). To sedate children usually younger than 6 years of age, oral chloral hydrate (50 mg/kg) was initially used and intravenous midazolam (0.1 mg/kg) or ketamine (1 mg/kg) was additionally administered as required.

The lowest possible tube voltage with minimal or no tube current saturation (tube current is expressed as being saturated when it exceeds the maximal limit of X-ray tube output) was chosen to maximize radiation dose efficiency and iodine contrast-to-noise ratio: thus, 70 kV was used in 56 patients, 80 kV in 15, 100 kV in 27 and 120 kV in 1. At the selected tube voltage, the tube current time product per rotation for retrospectively ECG-gated spiral scan and volume CT dose index for prospectively ECG-triggered sequential scan with or without additional respiratory triggering was determined by the combination of body weight and the size of cardiac shadow on scout image for the former [11] and combination of the cross-sectional area and mean body density for the latter [14], respectively. These values were entered before the scan range adjustment to maximize radiation dose reduction without degrading image quality [10].

**Table 1** Patient-related and radiation dose parameters according to cardiac computed tomography (CT) scan modes

	Cardiac CT scan mode		
	ECG-gated ( <i>n</i> =39)	Combined-triggered ( <i>n</i> =37)	ECG-triggered ( <i>n</i> =23)
Age	16.2±8.5 years	2.0±3.4 years	5.9±17.6 months
Body surface area (m <sup>2</sup> )	1.5±0.3	0.5±0.2	0.3±0.1
Volume CT dose index (mGy)	12.8±5.2	1.3±0.7	1.6±0.9
Dose-length product (mGy·cm)	348.5±197.8	18.8±10.6	13.3±7.5
Effective dose (mSv)	5.0±4.6	0.7±0.3	0.8±0.5

ECG electrocardiography

Iodinated contrast agent (Iomeron 400, iomeprol 400 mg I/ml; Bracco Imaging SpA, Milan, Italy; 1.5–2.0 ml/kg body weight) was intravenously administered using a dual-head power injector at an injection rate of 0.3–3.0 ml/s depending on the sizes of the body and the placed angiocatheter. A triphasic injection protocol, in which undiluted contrast agent was followed by 50% diluted contrast agent and then by 5% diluted contrast agent, was utilized for retrospectively ECG-gated spiral and prospectively ECG-triggered sequential scans to achieve uniform cardiovascular enhancement and minimal perivenous streak artifacts from undiluted contrast agent. On the other hand, a quadriphasic injection protocol with decremental injection rates was utilized for the prospectively combined ECG- and respiratory-triggered sequential scan to lengthen the peak vascular enhancement time required for a longer total scan time as follows: the first two phases of the undiluted contrast agent were followed by a third phase of 50% diluted contrast agent and then by a fourth phase of 5% diluted contrast agent; injection rates were gradually diminished by 0.1–0.2 ml/s, mandatorily between the first and second phases and optionally between the other phases [13]. The scan delay time was determined by a bolus tracking technique with a trigger threshold of 150 Hounsfield units (HU) in the left ventricular cavity.

After cardiac CT scanning, volume CT dose index and dose-length product (DLP) values based on a 32-cm phantom were automatically recorded and stored in our picture archiving and communication system. The effective dose values of cardiac CT were calculated by multiplying the DLP times the age, gender and tube voltage-specific conversion factors for chest CT [15].

### Quantification of left ventricular volumes and masses

The stacks of thin sections from axial cardiac CT scans were sent to a commercially available workstation (Advantage Windows 4.6; GE Healthcare, Milwaukee, WI) for image evaluation. For the quantification of left ventricular volumes and masses, a semiautomatic 3-D threshold-based

segmentation method in which the papillary muscles and trabeculations were excluded from the ventricular cavity (Fig. 1) was used. The epicardial border of the left ventricle was outlined serially using one-click identification of the left ventricle, 3-D region-growing method and manual adjustment. In addition, manual adjustment was necessary to define the mitral and aortic valve planes accurately. Furthermore, the coronary arteries and cardiac veins in the left ventricular myocardium were excluded from the total left ventricular volume by applying a visually determined threshold. Left ventricular cavity volume was subsequently obtained by applying a threshold to the total left ventricular volume. An optimal segmentation threshold was determined to separate the most compact interventricular septal myocardium from adjacent ventricular blood for each cardiac phase by using a histogram-assisted analysis to reduce visual perception errors [9–11, 16]. The left ventricular mass (cm<sup>3</sup> or ml) was subsequently calculated by subtracting the ventricular cavity volume from the total ventricular volume for each cardiac phase (Fig. 1). The value was subsequently multiplied by the specific gravity of the myocardium (1.05 g/ml or g/cm<sup>3</sup>).

The preliminary volumetric segmentation was conducted by a radiology technologist with 8 years of experience in cardiac CT image processing and the final result was validated by a radiologist (H.W.G) with 18 years of experience in cardiac CT. It was also evaluated whether the volumetric measurements were inaccurate because of heterogeneous or insufficient contrast enhancement of left ventricular blood, a streak artifact from less diluted contrast agent or a metal artifact, among other reasons. The volumetric parameters were indexed to body surface area. Post-processing time was recorded for each cardiac phase. In addition, both left ventricular mass-volume and volume-mass ratios were calculated for each cardiac phase because both of them have been used for evaluating left ventricular hypertrophy or remodeling in the literature [17–20].

The technical feasibility of the method used for left ventricular mass quantification was considered to be present when any failures in data uploading and data segmentation occurred in more than 10% of cases, and when the measurements were reproducible with mean differences between two separate evaluations of less than 10%. To evaluate the reproducibility

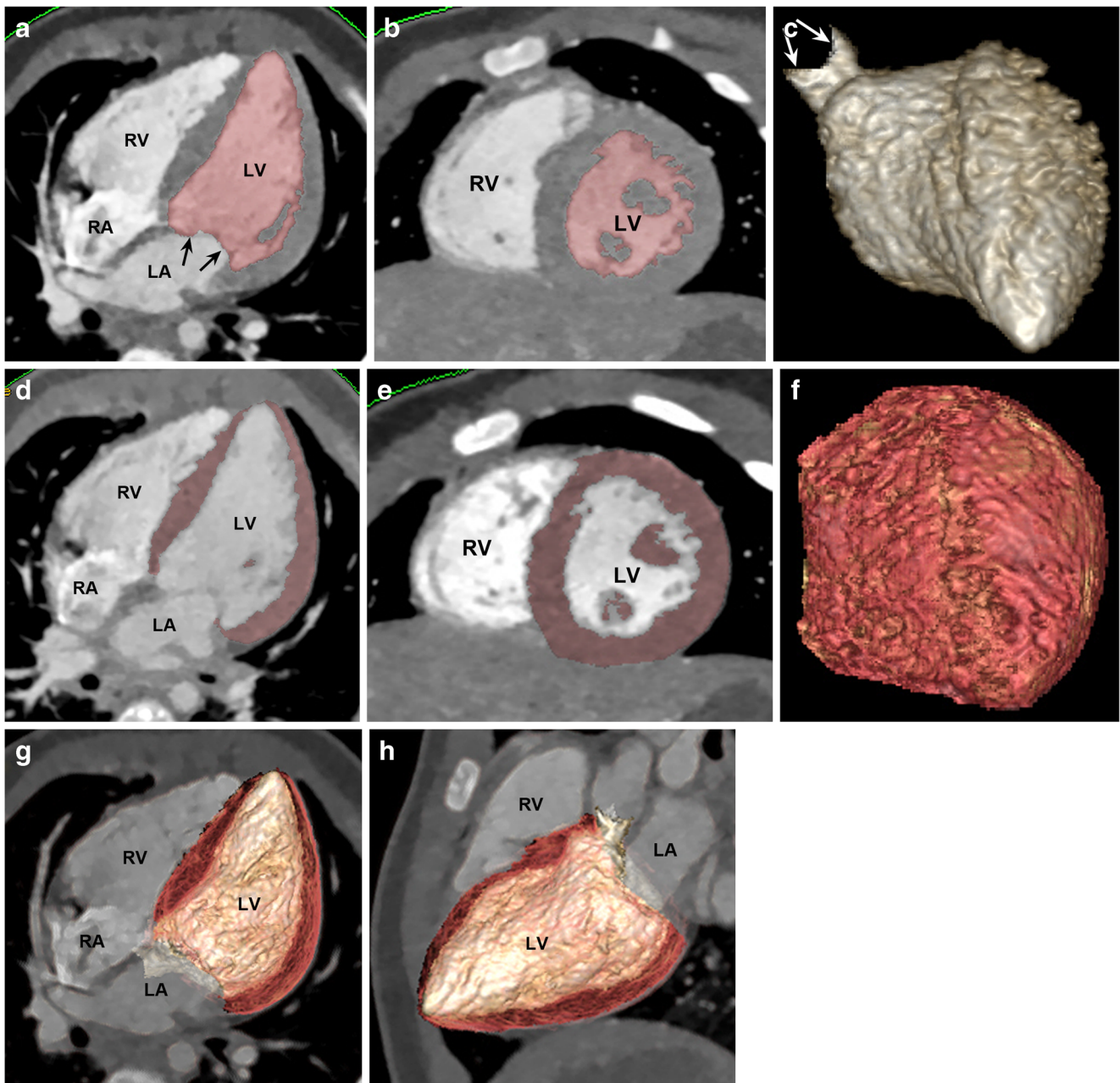


**Fig. 1** Left ventricular mass and volume quantification using the semiautomatic 3-D threshold-based cardiac CT segmentation method in an 1-year-old girl with repaired interrupted aortic arch. **a, b** Four-chamber (**a**) and short-axis (**b**) end-diastolic cardiac CT images show the segmented left ventricular cavity in pink after threshold-based exclusion of the papillary muscles and trabeculations of the left ventricle. The mitral valve plane (*arrows*) was manually adjusted. **c** Anterior 3-D image illustrates the segmented left ventricular cavity volume. The measured left ventricular end-diastolic volume was 31.6 ml. The aortic valve plane (*arrows*) was manually corrected. **d, e** Four-chamber (**d**) and short-axis (**e**) end-diastolic cardiac CT images demonstrate the

segmented left ventricular mass in pink after threshold-based inclusion of the papillary muscles and trabeculations of the left ventricle. **f** Anterior 3-D image illustrates the segmented left ventricular myocardial mass. Irregular surface of the myocardial mass is a result of the exclusion of the coronary arteries and cardiac veins from the left ventricular myocardium. **g, h** Inferior (**g**) and left lateral (**h**) images generated by merging 2-D multiplanar and 3-D segmented images illustrate the segmented left ventricular volume (light pink) and mass (purple) together. *LA* left atrium, *LV* left ventricle, *RA* right atrium, *RV* right ventricle

of quantification of the left ventricular mass, the two same observers blinded to the initial results quantified the left ventricular mass more than 1 year later. The mean differences between the two sessions were calculated.

### Left ventricular hypertrophy

A quantitative diagnostic criterion of left ventricular hypertrophy, e.g., the 95th percentile value estimated from healthy

subjects, was not available for the segmentation method used in this study. Therefore, the degree of left ventricular hypertrophy was assessed visually on cardiac CT and echocardiographic images, and was categorized into definite hypertrophy, borderline hypertrophy, and no hypertrophy groups.

### Statistical analysis

Continuous variables are presented as mean±standard deviation or median with range, and categorical variables are expressed as frequency with percentage. Continuous variables were compared between the two groups by using the unpaired *t*-test. The one-way analysis of variance with Tukey honest significant difference post-hoc test or Kruskal-Wallis test was utilized to compare the three group means. The paired *t*-test was utilized to compare the means of paired continuous variables. The degree of correlation between the paired continuous variables was analyzed by calculating the Pearson correlation coefficient. A *P*-value of less than 0.05 was considered statistically significant. Statistical analyses were performed by using statistical software (SPSS version 24.0; IBM Corp., Armonk, NY, USA).

### Results

All left ventricular volumetric measurements from cardiac CT data could be successfully obtained without any failures including data uploading and data segmentation. The body surface area of 99 patients at cardiac CT exam was  $0.8\pm 0.6$  m<sup>2</sup>. Volume CT dose index, DLP and effective dose of cardiac CT in the 99 patients were  $5.9\pm 6.5$  mGy,  $147.4\pm 204.4$  mGy·cm and  $2.4\pm 3.5$  mSv, respectively, which were quite variable due to the use of ECG-gating or ECG-triggering for CT scanning.

#### Left ventricular volumetric measurements

Indexed end-systolic volume, indexed end-systolic mass, end-systolic volume-mass ratio, and end-systolic mass-volume ratio in 95 patients were  $27.8\pm 25.5$  ml/m<sup>2</sup>,  $72.8\pm 33.0$  g/m<sup>2</sup>,  $0.4\pm 0.3$  ml/g and  $4.2\pm 3.2$  g/ml, respectively. Indexed end-diastolic volume, indexed end-diastolic mass, end-diastolic volume-mass ratio and end-diastolic mass-volume ratio in 25 patients were  $71.0\pm 45.1$  ml/m<sup>2</sup>,  $65.3\pm 42.5$  g/m<sup>2</sup>,  $1.2\pm 0.6$  ml/g, and  $1.0\pm 0.5$  g/ml, respectively. Indexed mid-diastolic masses in 3 patients were 52.6, 56.1, and 128.5 g/m<sup>2</sup>, respectively.

In 24 patients who underwent end-systolic and end-diastolic cardiac CT, the indexed mass values obtained at the end-systolic phase were significantly higher than those obtained at the end-diastolic phase ( $71.4\pm 42.9$  g/m<sup>2</sup> vs.  $65.9\pm 43.3$  g/m<sup>2</sup>, *P*<0.001); the paired indexed masses obtained at the two cardiac phases showed a very high correlation (*R*=0.99, *P*<0.001) (Fig. 2). The quantification method of the left

ventricular mass used in this study exhibited high reproducibility with a mean difference between the two evaluation sessions of  $2.3\pm 1.1\%$ .

#### Cardiac CT scan mode

Patient-related and radiation dose parameters of cardiac CT scan modes are described in Table 1. Patient age, volume CT dose index, DLP and effective dose showed no statistically significant differences between prospectively combined ECG- and respiratory-triggered sequential scan and prospectively ECG-triggered sequential scan (*P*>0.05) (Table 1). In contrast, body surface area showed statistically significant differences among the three scan modes (*P*≤0.003) (Table 1); in the group with retrospectively ECG-gated spiral scan, age, volume CT dose index, DLP and effective dose were statistically significantly higher than those in the two groups with prospectively ECG-triggered sequential scan with or without additional respiratory triggering (*P*<0.001) (Table 1).

#### Left ventricular hypertrophy

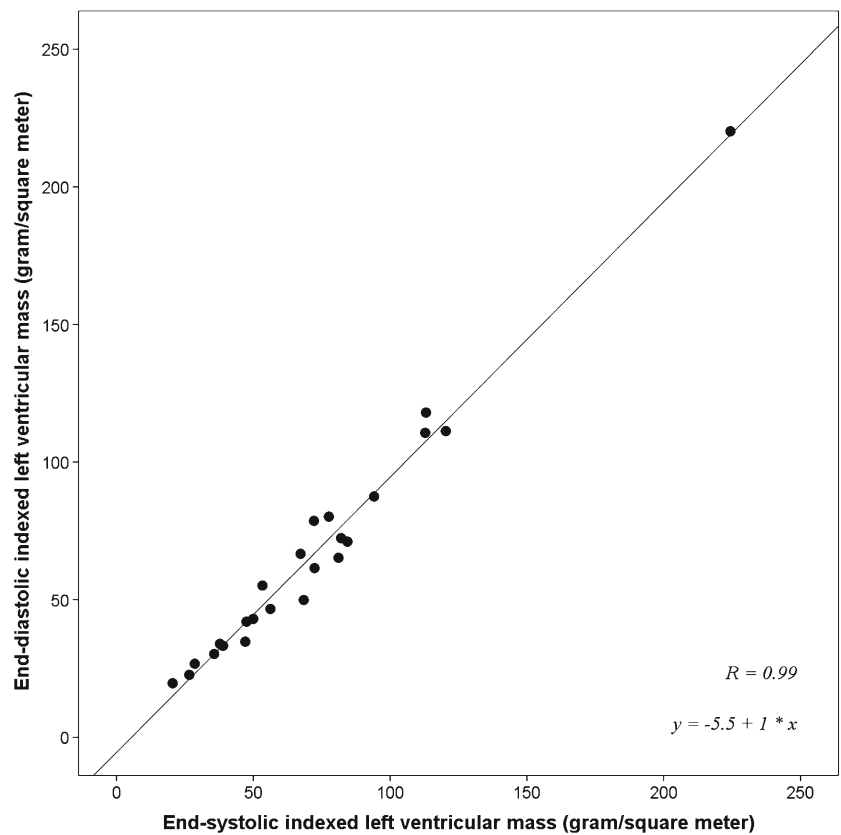
Patient-related parameter, indexed left ventricular mass and left ventricular volume-mass and mass-volume ratios of three (i.e. definite, borderline and none) left ventricular hypertrophy groups are described in Table 2. No statistically significant differences in age and body surface area were found among the three groups (*P*>0.05) (Table 2). The definite left ventricular hypertrophy group (Fig. 3) showed statistically significant higher indexed mass values than the borderline and no left ventricular hypertrophy groups (*P*<0.03), while there was no statistically significant difference in indexed mass between the borderline and no left ventricular hypertrophy groups (*P*>0.05) (Table 2).

The end-systolic volume-mass ratio showed statistically significant differences among the three left ventricular hypertrophy groups (*P*≤0.002) (Table 2). The definite left ventricular hypertrophy group demonstrated statistically significant higher end-systolic mass-volume ratios than the borderline and no left ventricular hypertrophy groups (*P*<0.001), whereas there was no statistically significant difference between the borderline and no left ventricular hypertrophy groups (*P*>0.05) (Table 2). The end-diastolic volume-mass and mass-volume ratios showed statistically significant differences among the three left ventricular hypertrophy groups (*P*<0.001) (Table 2).

#### Post-processing time

The post-processing time for cardiac CT left ventricular volumetry was  $11.6\pm 1.6$  min for the end-systolic phase (*n*=95) and  $13.4\pm 1.9$  min for the end-diastolic phase (*n*=25). In 24 patients with paired end-systolic and end-diastolic data

**Fig. 2** Scatter plot between indexed end-systolic and end-diastolic left ventricular myocardial mass values. Pearson correlation coefficient of the scatter plot was 0.99, indicating a very high positive linear correlation between the paired indexed left ventricular mass values obtained at the end-systolic and end-diastolic phases



sets, the post-processing time of the end-diastolic data set ( $13.4 \pm 1.9$  min) was statistically significantly longer than that of the end-systolic data set ( $12.7 \pm 1.4$  min,  $P < 0.02$ ).

**Discussion**

This study demonstrated that the semiautomatic 3-D threshold-based cardiac CT segmentation method was technically feasible with high reproducibility for left ventricular mass quantification in patients with various degrees of left ventricular hypertrophy. As a result, the segmentation method could reduce underestimation of left ventricular mass caused by 2-D contouring methods. The method showed high reproducibility

in quantifying left ventricular mass because user interactions producing intricate endocardial borders could be minimized. This advantage appears particularly beneficial in a subset of cardiac diseases, such as hypertrophic cardiomyopathy, myocardial non-compaction and Fabry disease [21–24]. The absence of technical failures in this study might be attributed to excellent image quality of cardiac CT images. On the contrary, cardiac MRI is often susceptible to inhomogeneous signal intensity, flow-related artifacts and metal artifacts [16], which may lead to a technical failure of a threshold-based segmentation method.

Traditionally, left ventricular mass is calculated at the end-diastole [25]. The myocardial volume and weight theoretically should be almost constant irrespective of cardiac phases. In

**Table 2** Patient-related and left ventricular volumetric parameters according to the degree of left ventricular hypertrophy

	Left ventricular hypertrophy		
	Definite	Borderline	None
Age (years)	6.4±12.4 (n=34)	8.8±10.3 (n=35)	11.4±10.7 (n=30)
Body surface area (m <sup>2</sup> )	0.6±0.5 (n=34)	0.9±0.6 (n=35)	1.0±0.6 (n=30)
Indexed mass (g/m <sup>2</sup> )	83.5±41.3 (n=41)	64.7±26.9 (n=42)	55.6±23.9 (n=40)
End-systolic volume/mass ratio (ml/g)	0.2±0.1 (n=34)	0.4±0.1 (n=33)	0.7±0.4 (n=28)
End-diastolic volume/mass ratio (ml/g)	0.7±0.2 (n=7)	1.1±0.3 (n=8)	1.7±0.7 (n=10)
End-systolic mass-volume ratio (ml/g)	7.3±3.4 (n=34)	2.9±0.8 (n=33)	1.8±0.8 (n=28)
End-diastolic mass-volume ratio (ml/g)	1.5±0.4 (n=7)	1.0±0.2 (n=8)	0.7±0.2 (n=10)

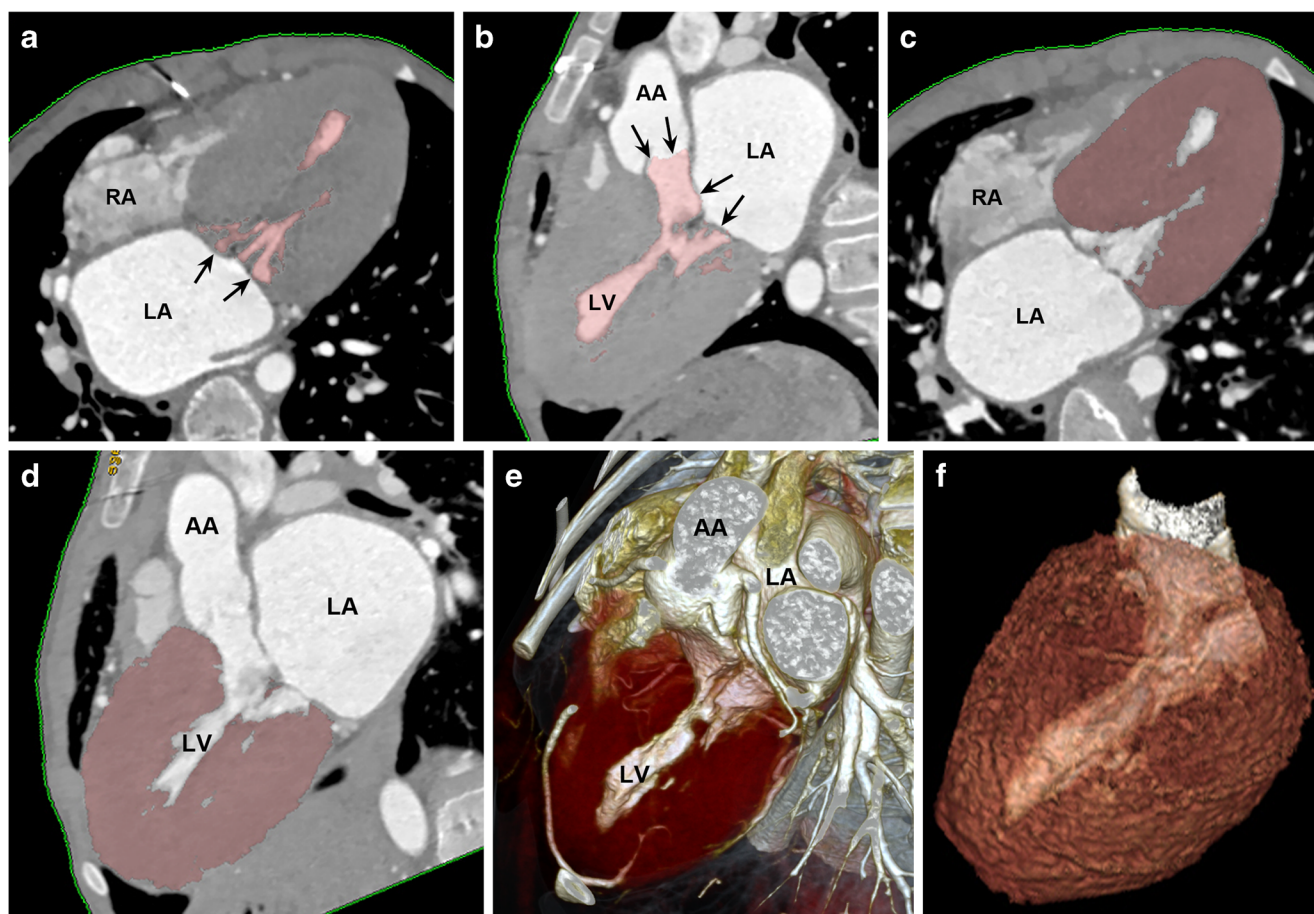


**Fig. 3** Left ventricular mass and volume quantification using the semiautomatic 3-D threshold-based cardiac CT segmentation method in an 11-year-old boy with hypertrophic cardiomyopathy. **a, b** Four-chamber (**a**) and left ventricular outflow (three-chamber) (**b**) end-systolic cardiac CT images show the segmented left ventricular cavity in pink after threshold-based exclusion of the papillary muscles and trabeculations of the left ventricle. The mitral and aortic valve planes (*arrows*) were manually adjusted. The enlarged left atrium with mitral valve thickening is noted. **c, d** Four-chamber (**c**) and left ventricular outflow (three-chamber) (**d**) end-systolic cardiac CT images demonstrate the segmented left ventricular mass in pink after threshold-

based inclusion of the papillary muscles and trabeculations of the left ventricle. The left ventricular myocardium appears concentrically hypertrophic and this case was visually graded as definite left ventricular hypertrophy group. **e, f** Left lateral unsegmented (**e**) and segmented (**f**) volume-rendered cardiac CT images equally illustrate the left ventricular cavity (light pink) and myocardium (sepia) simultaneously. However, only the segmented image data could provide the measured left ventricular cavity volume (17.7 ml) and the measured left ventricular myocardial mass (217.7 g). AA ascending aorta, LA left atrium, LV left ventricle, RA right atrium

previous studies [26, 27] comparing left ventricular mass between the end-systolic, mid-diastolic and end-diastolic phase CT data sets, the end-systolic phase showing the least trabeculated ventricular myocardium and the greatest left ventricular mass values is recommended. The differences in left ventricular mass among different cardiac phases are (less than 4–5%) and high correlations ( $r=0.95$ – $0.98$ ) are coherently demonstrated [26, 27]. This study also showed a small difference of 7.7% and high correlation of 0.99 between the left ventricular masses measured at the end-systolic and end-diastolic phases.

The slightly smaller end-diastolic left ventricular mass in this study might be closely linked to the slightly overestimated end-diastolic left ventricular volume due to the partial volume effect. On this occasion, a partial voxel interpolation technique

can minimize this partial volume effect, thereby increasing the accuracy of left ventricular mass quantification [28].

Ex vivo validation of left ventricular mass measured by 2-D short-axis cine MRI was reported in animal hearts [28] and excised human hearts after transplantation [29]. Although it is difficult to conduct and has its own pitfalls, similar ex vivo validation would be helpful to back up the accuracy of cardiac CT for left ventricular mass quantification. In left ventricular mass quantified by cardiac CT, low interscan variability was reported [30]; this study also exhibited a small mean difference of 2.3% between the two evaluations.

Left ventricular hypertrophy, as a remodeling or adaptation to overloaded conditions, may be classified as concentric, eccentric or asymmetric [18]. Therefore, it is taken for granted that left ventricular mass estimated by M-mode

echocardiography evaluating only a 1-D view is likely inaccurate [3, 31]. In this respect, left ventricular mass needs to be accurately quantified and the papillary muscles and trabeculations should be included in the left ventricular myocardium using the 3-D threshold-based segmentation method. Left ventricular hypertrophy is quantitatively defined as indexed left ventricular mass generally greater than the 95th percentile value estimated from normal subjects. Gender-specific normal reference values have been reported for cardiac MRI [32–34] and cardiac CT [26, 30, 35]. However, such values are lacking for the proposed cardiac CT segmentation method evaluated in this study. Therefore, left ventricular hypertrophy had to be visually graded. Nonetheless, the definite left ventricular hypertrophy group showed significantly higher indexed mass values than the borderline and no left ventricular hypertrophy groups.

Left ventricular volume-mass or mass-volume ratio has been used to evaluate ventricular remodeling, diastolic function, hypertrophic cardiomyopathy, and hypertensive response to exercise [17–20]. In this study, such ratios could be calculated from the CT-measured ventricular volumes and masses. Further studies are necessary to define the clinical utility of these CT-based ratios demonstrated in this study.

The cardiac CT radiation dose was thoroughly optimized in this study (0.7–5.0 mSv) by utilizing various dose-reduction strategies [10, 11, 14, 15]. A previous study also demonstrated that prospectively ECG-triggered sequential scan (6.2 mSv) could dramatically reduce radiation dose in quantifying ventricular function and mass in 20 adults compared with retrospectively ECG-gated spiral scan (28.6 mSv) [36]. In this study, three scan modes had to be used to cover children with different body sizes and levels of cooperation seamlessly; prospectively combined ECG- and respiratory-triggered sequential scan is an indispensable imaging technique enabling ventricular function assessment in free-breathing young children [12, 13].

Post-processing time (11.6–13.4 min) of the semiautomatic 3-D threshold-based cardiac CT segmentation method in this study is longer than those of automated 3-D cardiac CT segmentation methods in the range of 3.4–10.0 min [35, 37], which is a major limitation of the methodology for clinical utility. However, as suggested in a previous study [7], additional time for epicardial border tracing would be relatively short and expected to be even shorter if utilizing a more time-efficient algorithm in the future. Notably, the additional time investment allows us to utilize an ample set of ventricular volumetric parameters, including ventricular volume, myocardial mass, and volume-mass and mass-volume ratios.

This study has several limitations. First, there is no in vivo reference method to validate the measured left ventricular myocardial mass values. Nevertheless, closely correlated left ventricular mass values among the different cardiac phases in this study and other studies [26, 27, 30] may partly support a

favorable precision of the CT-based algorithms. Second, a less accurate subjective grading of left ventricular hypertrophy was used because normal values utilizing the same cardiac CT segmentation method are not available. This study, however, could demonstrate that the definite left ventricular hypertrophy group had significantly greater left ventricular mass than the other two groups. Third, the proposed method for left ventricular mass quantification should be tested by other investigators because it was a single institution's experience. Last, its clinical value should be defined in further studies for homogeneous patient populations with a specific cardiac disease although several potentials were demonstrated in this study.

## Conclusion

CT quantification of left ventricular mass using semiautomatic 3-D threshold-based segmentation is feasible with high reproducibility and the mass values and its ratios with ventricular volumes may be used in patients with various degrees of left ventricular hypertrophy.

## Compliance with ethical standards

**Conflicts of interest** None

## References

1. Stevens SM, Reinier K, Chugh SS (2013) Increased left ventricular mass as a predictor of sudden cardiac death: is it time to put it to the test? *Circ Arrhythm Electrophysiol* 6:212–217
2. Armstrong AC, Gjesdal O, Almeida A et al (2014) Left ventricular mass and hypertrophy by echocardiography and cardiac magnetic resonance: the multi-ethnic study of atherosclerosis. *Echocardiography* 31:12–20
3. Avegliano GP, Costabel JP, Asch FM et al (2016) Utility of real time 3D echocardiography for the assessment of left ventricular mass in patients with hypertrophic cardiomyopathy: comparison with cardiac magnetic resonance. *Echocardiography* 33:431–436
4. Chuang ML, Gona P, Hautvast GL et al (2012) Correlation of trabeculae and papillary muscles with clinical and cardiac characteristics and impact on CMR measures of LV anatomy and function. *JACC Cardiovasc Imaging* 5:1115–1123
5. Varga-Szemes A, Muscogiuri G, Schoepf UJ et al (2016) Clinical feasibility of a myocardial signal intensity threshold-based semi-automated cardiac magnetic resonance segmentation method. *Eur Radiol* 26:1503–1511
6. Sugeng L, Mor-Avi V, Weinert L et al (2010) Multimodality comparison of quantitative volumetric analysis of the right ventricle. *JACC Cardiovasc Imaging* 3:10–18
7. Kim HJ, Goo HW, Park SH, Yun TJ (2013) Left ventricle volume measured by cardiac CT in an infant with a small left ventricle: a new and accurate method in determining uni- or biventricular repair. *Pediatr Radiol* 43:243–246
8. Goo HW, Park S (2015) Semiautomatic three-dimensional CT ventricular volumetry in patients with congenital heart disease:



- agreement between two methods with different user interaction. *Int J Card Imaging* 31:223–232
9. Goo HW (2017) Serial changes in anatomy and ventricular function on dual-source cardiac computed tomography after the Norwood procedure for hypoplastic left heart syndrome. *Pediatr Radiol* 47:1776–1786
  10. Goo HW (2018) Is it better to enter a volume CT dose index value before or after scan range adjustment for radiation dose optimization of pediatric cardiothoracic CT with tube current modulation? *Korean J Radiol* 19:692–703
  11. Goo HW (2018) Comparison of chest pain protocols for electrocardiography-gated dual-source cardiothoracic CT in children and adults: the effect of tube current saturation on radiation dose reduction. *Korean J Radiol* 19:23–31
  12. Goo HW, Allmendinger T (2017) Combined electrocardiography- and respiratory-triggered CT of the lung to reduce respiratory misregistration artifacts between imaging slabs in free-breathing children: initial experience. *Korean J Radiol* 18:860–866
  13. Goo HW (2018) Combined prospectively electrocardiography- and respiratory-triggered sequential cardiac computed tomography in free-breathing children: success rate and image quality. *Pediatr Radiol* 48:923–931
  14. Goo HW (2011) Individualized volume CT dose index determined by cross-sectional area and mean density of the body to achieve uniform image noise of contrast-enhanced pediatric chest CT obtained at variable kV levels and with combined tube current modulation. *Pediatr Radiol* 41:839–847
  15. Goo HW (2012) CT radiation dose optimization and estimation: an update for radiologists. *Korean J Radiol* 13:1–11
  16. Goo HW (2018) Comparison between three-dimensional navigator-gated whole-heart MRI and two-dimensional cine MRI in quantifying ventricular volumes. *Korean J Radiol* 19:704–714
  17. Buakhamsri A, Popovic ZB, Lin J et al (2009) Impact of left ventricular volume/mass ratio on diastolic function. *Eur Heart J* 30:1213–1221
  18. Dweck MR, Joshi S, Murigu T et al (2012) Left ventricular remodeling and hypertrophy in patients with aortic stenosis: insights from cardiovascular magnetic resonance. *J Cardiovasc Magn Reson* 14:50
  19. Krieger EV, Clair M, Opatowsky AR et al (2013) Correlation of exercise response in repaired coarctation of the aorta to left ventricular mass and geometry. *Am J Cardiol* 111:406–411
  20. Luijkx T, Cramer MJ, Buckens CF et al (2015) Unravelling the grey zone: cardiac MRI volume to wall mass ratio to differentiate hypertrophic cardiomyopathy and the athlete's heart. *Br J Sports Med* 49:1404–1409
  21. Han Y, Osborn EA, Maron MS et al (2009) Impact of papillary and trabecular muscles on quantitative analyses of cardiac function in hypertrophic cardiomyopathy. *J Magn Reson Imaging* 30:1197–1202
  22. Park EA, Lee W, Kim HK, Chung JW (2015) Effect of papillary muscles and trabeculae on left ventricular measurement using cardiovascular magnetic resonance imaging in patients with hypertrophic cardiomyopathy. *Korean J Radiol* 16:4–12
  23. Jacquier A, Thuny F, Jop B et al (2010) Measurement of trabeculated left ventricular mass using cardiac magnetic resonance imaging in the diagnosis of left ventricular non-compaction. *Eur Heart J* 31:1098–1104
  24. Kozor R, Callaghan F, Tchan M et al (2015) A disproportionate contribution of papillary muscles and trabeculations to total left ventricular mass makes choice of cardiovascular magnetic resonance analysis technique critical in Fabry disease. *J Cardiovasc Magn Reson* 17:22
  25. Schwarz F, Takx R, Schoepf UJ et al (2011) Reproducibility of left and right ventricular mass measurements with cardiac CT. *J Cardiovasc Comput Tomogr* 5:317–324
  26. Mao SS, Li D, Rosenthal DG et al (2013) Dual-standard reference values of left ventricular volumetric parameters by multidetector CT angiography. *J Cardiovasc Comput Tomogr* 7:234–240
  27. Klein R, Ametepé ES, Yam Y et al (2017) Cardiac CT assessment of left ventricular mass in mid-diastasis and its prognostic value. *Eur Heart J Cardiovasc Imaging* 18:95–102
  28. Codella NC, Lee HY, Fieno DS et al (2012) Improved left ventricular mass quantification with partial voxel interpolation: in vivo and necropsy validation of a novel cardiac MRI segmentation algorithm. *Circ Cardiovasc Imaging* 5:137–146
  29. Farber NJ, Reddy ST, Doyle M et al (2014) Ex vivo cardiovascular magnetic resonance measurements of right and left ventricular mass compared with direct mass measurement in excised hearts after transplantation: a first human SSFP comparison. *J Cardiovasc Magn Reson* 16:74
  30. Budoff MJ, Ahmadi N, Sarraf G et al (2009) Determination of left ventricular mass on cardiac computed tomographic angiography. *Acad Radiol* 16:726–732
  31. Supe-Markovina K, Nielsen JC, Musani M et al (2016) Assessment of left ventricular mass and hypertrophy by cardiovascular magnetic resonance imaging in pediatric hypertension. *J Clin Hypertens (Greenwich)* 18:976–981
  32. Robbers-Visser D, Boersma E, Helbing WA (2009) Normal biventricular function, volumes, and mass in children aged 8 to 17 years. *J Magn Reson Imaging* 29:552–559
  33. Sarikevich S, Peters B, Gutberlet M et al (2010) Sex-specific pediatric percentiles for ventricular size and mass as reference values for cardiac MRI: assessment by steady-state free-precession and phase-contrast MRI flow. *Circ Cardiovasc Imaging* 3:65–76
  34. Kawel-Boehm N, Maceira A, Valsangiacomo-Buechel ER et al (2015) Normal values for cardiovascular magnetic resonance in adults and children. *J Cardiovasc Magn Reson* 17:29
  35. Stojanovska J, Prasitdumrong H, Patel S et al (2014) Reference absolute and indexed values for left and right ventricular volume, function and mass from cardiac computed tomography. *J Med Imaging Radiat Oncol* 58:547–558
  36. Takx RA, Moscariello A, Schoepf UJ et al (2012) Quantification of left and right ventricular function and myocardial mass: comparison of low-radiation dose 2nd generation dual-source CT and cardiac MRI. *Eur J Radiol* 81:e598–e604
  37. Kara B, Nayman A, Guler I et al (2016) Quantitative assessment of left ventricular function and myocardial mass: a comparison of coronary CT angiography with cardiac MRI and echocardiography. *Pol J Radiol* 81:95–102